Conversion of Hydrogen-bonded Manganese(II) and Zinc(II) Squarate ($C_4O_4^{2-}$) Molecules, Chains and Sheets to Three-dimensional Cage Networks†

Omar M. Yaghi,* Guangming Li and Thomas L. Groy
Department of Chemistry and Biochemistry, Goldwater Center for Science and Engineering, Arizona State University, Tempe, Arizona 85287, USA

Very strong hydrogen-bonding interactions can be utilized to guide the assembly of the molecular building block $[Mn(HC_4O_4)_2(OH_2)_4]$ ($H_2C_4O_4$ = squaric acid, 3,4-dihydroxycyclobut-3-ene-1,2-dione) in the crystal. X-Ray structural analysis of these crystals [triclinic, $P\bar{1}$, a = 5.1910(4), b = 7.4605(7), c = 8.9088(11) Å, α = 67.07(1), β = 77.23(1), γ = 74.49(1)°, Z = 1] revealed the presence of two very short hydrogen-bonding contacts, O–H ··· O = 2.464(1) and 2.481(1) Å, which are responsible for the formation of chains and sheets of manganese squarates(1−) in the crystal. Additional hydrogen-bonding contacts that are weaker but numerous are present and they lead to the formation of a strongly associated three-dimensional manganese squarate(1−) network. The complexity of this hydrogen-bonding pattern was simplified by substituting, in the zinc analogue, two water molecules with dmso (dmso = dimethyl sulfoxide) to give $[Zn(C_4O_4)(OH_2)_2(dmso)_2]$, which was characterized by single-crystal X-ray diffraction [monoclinic, $P2_1/c$, a = 15.697(6), b = 8.116(4), c = 12.211(5) Å, β = 115.83(3)°, Z = 4]. Here, extended chains of zinc squarate are present and found to be linked together by hydrogen bonds to form a layered solid. Further growth of this structure to produce a three-dimensional framework was prevented by virtue of the dmso ligands occupying axial positions at the zinc centre. The ability of the hydrogen bonds to act collectively over a large surface area of these solids adds to their overall crystal stability, as these compounds are insoluble at room temperature in aqueous and non-aqueous media. However, in aqueous media at 25–100 °C they undergo conversion reactions leading to the known extended three-dimensional cage network $M(C_4O_4)(OH_2)_2$ (M = Mn or Zn).

Designing solid-state materials that exhibit structure-function correlation requires knowledge of the relative orientation of the physically or chemically active components, with respect to each other, in the solid framework. However, this has been one of the most difficult aspects to control in materials synthesis, mainly due to the vast number of possible orientations a molecule may possess in the crystal lattice.[1] In an effort to develop and understand effective strategies for the achievement of structural control in the solid state, we have used symmetry and chemical functionality in the directed synthesis of a microporous three-dimensional channel network.[2] In this report, we show how hydrogen-bonding interactions can also guide and control the geometric association of molecular metal co-ordination complexes leading to stable extended networks. Given the directional, selective and attractive nature of these interactions and their demonstrated utility in molecular-recognition systems,[3] it is reasonable to anticipate their applicability to the directed assembly of co-ordination solids. This study was initiated by focusing on hydrogen-bonding patterns between specific functional groups and metal ion centres; two simple molecular building blocks were chosen, namely, transition metal aqua ions and squaric acid (3,4-dihydroxycyclobut-3-ene-1,2-dione, $H_2C_4O_4$). This is for at least two reasons: the symmetrical, planar and rigid properties of the squarate provide a minimal amount of hindrance to hydrogen bonds originating from the metal centre; the small size of water coupled to its strong hydrogen-bonding capabilities contribute largely to crystal stability. Here we describe the synthesis, structure and properties of $[Mn(HC_4O_4)_2(OH_2)_4]$, a hydrogen-bonded three-dimensional molecular network containing one of the shortest hydrogen-bonding interactions known, and $[Zn(C_4O_4)(OH_2)_2(dmso)_2]$ (dmso = dimethyl sulfoxide), containing extended chains linked by hydrogen bonds to form a layered solid. The conversion of these compounds to the known three-dimensional extended cage network $M(C_4O_4)(OH_2)_2$ (M = Mn or Zn)[4] is presented.

† *Supplementary data available:* see Instructions for Authors, *J. Chem. Soc., Dalton Trans.*, 1995, Issue 1, pp. xxv–xxx.

Experimental

Materials and Methods.—All starting materials were purchased from commercial sources and used as received. Deionized water was used in all operations and manipulations of compounds. X-Ray single-crystal analysis of the zinc compound was performed by the Crystalytics Company (Lincoln, Nebraska). X-Ray powder diffraction (XRD) data are reported here for the most prominent lines with d spacings in Å and the relative intensities placed in parentheses. The homogeneity of the bulk products for all compounds prepared here was confirmed by comparison of the observed and calculated X-ray powder diffraction patterns. The calculated patterns were produced using the SHELXTL-XPOW program[5] with the single crystal data. Elemental analyses of products were performed on crystalline samples by the School of Chemical Sciences Microanalytical Laboratory at the University of Illinois-Urbana. Infrared spectra were measured from KBr pellets using a Nicolet FT-IR model Magna-IR system 550. Solid-state ^{13}C NMR spectra were recorded on a Varian UnitPlus-400 spectrometer by using a 7 mm cross-polarization magic angle spinning (CP MAS) probe and the chemical shifts were referenced externally to solid hexamethylbenzene.

Preparation of Compounds.—$[Mn(HC_4O_4)_2(OH_2)_4]$ **1**. When an equal volume aqueous mixture (20 cm^3) of $MnCl_2 \cdot 4H_2O$ (0.198 g, 1.00 mmol) and $H_2C_4O_4$ (0.228 g, 2.00 mmol) was allowed to stand in an uncovered container at room temperature for 2 d, pale pink crystals appeared. These were

filtered off and washed with 2 × 5 cm^3 of distilled water to give 0.21 g (60%) of product (Found: C, 27.30; H, 3.25; Mn, 14.70. $C_8H_{10}MnO_{12}$ requires C, 27.20; H, 2.85; Mn, 15.55%). IR (KBr, 1800–350 cm^{-1}): 1815m, 1630s, 1524m, 1125(sh), 1089s, 866m, 792w, 749w, 660(sh), 633m, 510(sh) and 372w cm^{-1}. Observed XRD: 6.816 (75), 4.976 (29), 4.661 (76), 4.487 (84), 4.213 (122), 4.020 (55), 3.383 (66), 3.090 (208), 2.604 (70) and 2.287 Å (34).

The zinc analogue was prepared in 62% yield (Found: C, 26.45; H, 2.80; Zn, 17.30. $C_8H_{10}O_{12}Zn$ requires C, 26.45; H, 2.75; Zn, 18.00%) by using this procedure and by employing $Zn(NO_3)_2{\cdot}6H_2O$ as a starting material.

$[Zn(C_4O_4)(OH_2)_2(dmso)_2]$ **2**. An equal volume of dmso solution mixture (20 cm^3) of $Zn(NO_3)_2{\cdot}6H_2O$ (0.298 g, 1.00 mmol) and $H_2C_4O_4$ (0.114 g, 1.00 mmol) was allowed to stand in an uncovered container for one week. Then rectangular colourless crystals appeared, which were filtered off and washed with 2 × 10 cm^3 of acetone, then dried in air to give 0.11 g, (30%) of product (Found: C, 26.25; H, 4.55; S, 16.45; Zn, 17.20. $C_8H_{16}O_8S_2Zn$ requires C, 26.00; H, 4.35; S, 17.35; Zn, 17.70%). IR (KBr, 1500–350 cm^{-1}): 1593w, 1560(sh), 1518s, 1400(sh), 1322w, 1110w, 1025m, 956m, 707w, 611m, 510(sh), 399w and 351w cm^{-1}. Observed XRD: 7.123 (179), 6.567 (105), 5.731 (323), 5.491 (89), 4.685 (41), 4.560 (43), 4.078 (41), 3.821 (63), 3.639 (104), 3.321 (44), 2.855 (52), 2.514 (45), 2.429 (36) and 2.358 Å (31).

$Zn(C_4O_4)(OH_2)_2{\cdot}0.2C_5H_5N$. This phase was prepared using a slightly modified version of a reported procedure.[4] An equal volume aqueous mixture of $H_2C_4O_4$ (0.114 g, 1.00 mmol) and $Zn(NO_3)_2{\cdot}6H_2O$ (0.298 g, 1.00 mmol) was neutralized to pH = 7 with pyridine (0.25 cm^3) to give a clear solution. Upon refluxing this solution at 80 °C for 24 h, cubic-like colourless crystals appeared. The mixture was cooled to room temperature and the crystals were collected and washed with 3 × 10 cm^3 of water then air dried overnight to give 0.181 g (79%) of product (Found: C, 25.30; H, 2.15; N, 1.20; Zn, 28.95. $C_5H_5N_{0.2}O_6Zn$ requires C, 26.20; H, 2.20; N, 1.20; Zn, 28.50%). IR (KBr, 1600–350 cm^{-1}): 1525s, 1110m, 880w, 808w, 762w, 722w, 676m, 558m and 426w. Observed XRD: 8.180 (100), 5.787 (75), 4.722 (33), 4.082 (270), 2.886 (17), 2.719 (39), 2.579 (15), 2.549 (31), 2.331 (13), 2.039 (25), 1.872 (12), 1.823 (12) and 1.570 Å (11). Calculated XRD (obtained by using single-crystal data reported in ref. 4): 8.146 (70), 5.822 (100), 4.806 (22), 4.073 (89), 2.911 (15), 2.768 (19), 2.490 (15), 2.335 (7), 2.037 (8), 1.851 (15), 1.807 (7) and 1.570 Å (7). ^{13}C CP MAS NMR (C_6Me_6): δ 121.5 (s, *m*-C_5H_5N), 133.9 (s, *p*-C_5H_5N), 148.7 (s, *p*-C_5H_5N) and 196.7 (s, C_4O_4).

Conversion Reactions.—$[Mn(HC_4O_4)_2(OH_2)_4] \longrightarrow Mn(C_4O_4)(OH_2)_2$. A pure crystalline sample of $[Mn(HC_4O_4)_2(OH_2)_4]$ (0.050 g, 0.142 mmol) was suspended in 5 cm^3 of water and heated to 100 °C. Most of the solid (90%) dissolved after 10 min and the resulting supernatant was filtered and allowed to cool to produce crystals of the starting material as confirmed by the X-ray powder diffraction pattern. However, the remaining small amount of solid filtrate from the original mixture had the same characteristic XRD pattern as that observed for $Zn(C_4O_4)(OH_2)_2{\cdot}0.2C_5H_5N$.

In a similar experiment, where solid $[Mn(HC_4O_4)_2(OH_2)_4]$ was placed in contact with water at 40 °C for 1 h, a 90% yield of $Mn(C_4O_4)(OH_2)_2$ was obtained. Its character was confirmed by the X-ray powder diffraction pattern which was coincident with that observed for $Zn(C_4O_4)(OH_2)_2{\cdot}0.2C_5H_5N$.

$[Zn(C_4O_4)(OH_2)_2(dmso)_2] \longrightarrow Zn(C_4O_4)(OH_2)_2$. A pure crystalline sample of $[Zn(C_4O_4)(OH_2)_2(dmso)_2]$ (0.053 g, 0.143 mmol) was suspended in 5 cm^3 of water for 30 min at room temperature, then filtered to give quantitatively a solid that showed the same characteristic XRD pattern as that observed for $Zn(C_4O_4)(OH_2)_2{\cdot}0.2C_5H_5N$.

X-Ray Crystallographic Studies of $[Mn(HC_4O_4)_2(OH_2)_4]$ **1** *and* $[Zn(C_4O_4)(OH_2)_2(dmso)_2]$ **2**.—Pale pink single crystals of complex **1** and colourless crystals of complex **2** suitable for X-ray diffraction studies were obtained in both cases by slow evaporation of their respective reaction mixtures at room temperature. Experimental details for the structure determinations of both complexes are given in Table 1. Photographic evidence confirmed that the cell for **2** is the proper one and not the corresponding half cell with the $P2_1/n$ space group.

Totals of 1062 (**1**) and 2237 (**2**) independent reflections having 2θ (Mo-Kα) < 50 (**1**) and 48.3° (**2**) were collected at 20 °C on a Siemens R3m/V autodiffractometer (**1**) or a Nicolet autodiffractometer (**2**) using full 1.40°-wide (**1**) and 2.40°-wide (**2**) ω scans and graphite-monochromated Mo-Kα radiation for approximately parallelepiped-shaped (**1** and **2**) specimens with dimensions of 0.20 × 0.22 × 0.25 mm (**1**) and 0.32 × 0.35 × 0.40 mm (**2**). Lattice parameters were obtained from least-squares analyses of 25 (**1**) and 15 (**2**) computer-centred reflections with 15 ≤ 2θ ≤ 30 and 2θ > 20°, respectively. The raw intensity data were converted to structure-factor amplitudes and their estimated standard deviations by correction for scan speed, background, and Lorentz and polarization effects using the XDISK facility within the SHELXTL PLUS program.[6] Empirical absorption corrections were applied to complex **2** using psi scans for 7 reflections in the scan range using the XEMP program.[7] Compound **1** crystallized in the triclinic system and statistics identified the space group as $P\bar{1}$ which was consistent with all stages of the subsequent structure determination and refinement, while compound **2** crystallized in the monoclinic system where systematic absences were consistent with the space group $P2_1/c$.

The structures were solved by direct methods with the Siemens SHELXTL PLUS[6] (**1**) or SHELXTL PC[8] (**2**) software packages. The resulting structural parameters have been refined to convergence using full-matrix least-squares techniques and a structural model which incorporated anisotropic thermal parameters for all non-hydrogen atoms and fixed isotropic thermal parameters for all hydrogen atoms. The asymmetric unit of compound **1** consists of one manganese atom located on a special position and one squarato(1−) ($HC_4O_4^-$) ligand in addition to two water molecules. The hydrogen atoms of the squarate monoanion were placed on the special positions, between adjacent squarate oxygens, while water hydrogens were placed at idealized positions with O–H = 0.85 Å. The asymmetric unit of compound **2** consists of two crystallographically distinct units, each composed of a zinc atom located on a special position, one-half of a squarate ($C_4O_4^{2-}$) and a dmso ligand and one water molecule. The water molecule hydrogen atoms H(1), H(2), H(21) and H(22) were located from a Fourier-difference map and refined as independent isotropic

Table 1 Crystallographic data for $[Mn(HC_4O_4)_2(OH_2)_4]$ **1** and $[Zn(C_4O_4)(OH_2)_2(dmso)_2]$ **2**

	1	**2**
Formula	$C_8H_{10}MnO_{12}$	$C_8H_{16}O_8S_2Zn$
M	353.10	369.70
Crystal system	Triclinic	Monoclinic
Space group	$P\bar{1}$	$P2_1/c$
a/Å	5.1910(4)	15.697(6)
b/Å	7.4605(7)	8.116(4)
c/Å	8.9088(11)	12.211(5)
α/°	67.07(1)	90.00
β/°	77.23(1)	115.83(3)
γ/°	74.49(1)	90
Z	1	4
U/Å^3	303.51(5)	1400(1)
D_c/g cm^{-3}	1.932	1.754
μ/mm^{-1}	1.108	2.08
F(000)	179	760
$R(F_o)$	0.023	0.032
$R'(F_o)$	0.038	0.039
Weighting scheme, w^{-1}	$\sigma^2(F) + 0.0002F^2$	$\sigma^2(F) + 0.0009F^2$

atoms. The four methyl groups [C(3), C(4), C(7), C(8) and their hydrogens] were refined as rigid rotors with sp^3 hybridized geometry and C–H = 0.96 Å.

In the last cycles of refinement for the structure of compound **1**, all parameters shifted by < 1% of the estimated standard deviations of the parameter and the final Fourier-difference map showed a largest difference peak of 0.36 e Å^{-3}. For compound **2**, the top four peaks of the final Fourier-difference map (0.84–0.44 e Å^{-3}) were within 1.05 Å of a zinc atom; there were no other peaks present above the background level of 0.36 e Å^{-3}. Final *R* factors are presented in Table 1.

Additional material available from the Cambridge Crystallographic Data Centre comprises H-atom coordinates, thermal parameters and remaining bond lengths and angles.

Results and Discussion

Structure of $[Mn(HC_4O_4)_2(OH_2)_4]$ **1**.—The reaction of manganese(II) or zinc(II) ions with $H_2C_4O_4$ in a 1:2 ratio in water at room temperature results in the formation of crystalline $[M(HC_4O_4)_2(OH_2)_4]$ (M = Mn or Zn). The two compounds were formulated on the basis of total elemental analysis. They are isomorphous as revealed by data obtained from their X-ray diffraction pattern.

The manganese compound was identified by a single-crystal X-ray structure determination, which revealed a hydrogen-bonded framework that is composed of a manganese disquarate (1 –) complex, shown in Fig. 1. This is the principal building block in the final solid-state structure. Hydrogen-bonding interactions with O–H ··· O < 2.80 Å will be considered in the discussion of structures reported here, as interactions longer than this are commonly considered weak.[9] Crystal data, atomic coordinates and selected bond lengths and angles are given in Tables 1, 2 and 3, respectively. The Mn^{II} lies in an almost perfect octahedron [O(1)–Mn–O(1a) = 180.0(1), O(6)–Mn–O(6a) = 180.0(1), O(5)–Mn–O(5a) = 180.0(1), O(1)–Mn–O(6) = 89.9(1), O(1)–Mn–O(5) = 91.9(1), O(5)–Mn–O(6) = 87.8(1)°] of four water molecules, and two $HC_4O_4^-$ ligands arranged in a *trans* configuration. This configuration is adopted by all metal squarates,[10] which might be due to unfavourable steric factors that are expected to arise with *cis* squarates. The positions of H(2) and H(3) lie on inversion centres relating adjacent building blocks. The respective positions of H(2) and H(3) on O(2) and O(3) are consistent with the observed elongation in C(2)–O(2) [1.281(2) Å] and C(3)–O(3) [1.268(2) Å] relative to the unprotonated C(4)–O(4) [1.232(2) Å]. The squarate monoanion is bound to the metal centre in the 1,3-bridging mode rather than the η^2-chelation mode, mainly due to the steric strain that is expected to result from the latter situation. In fact, there are no structurally characterized examples of this chelating co-ordination mode. In almost all known transition-metal squarate complexes the bidentate 1,3-bridging co-ordination has been observed.

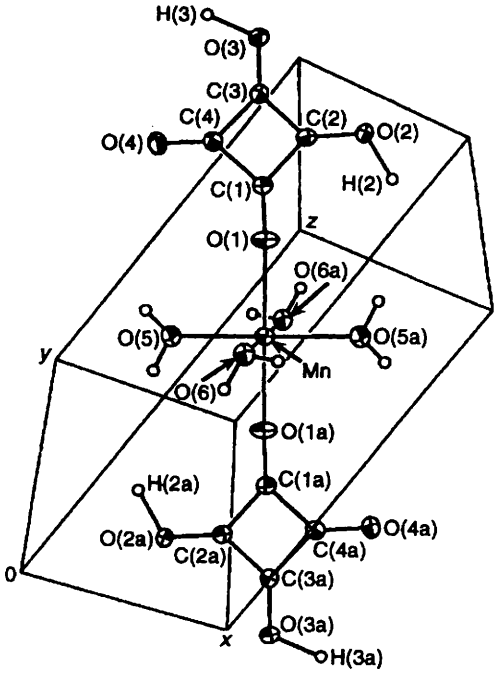

Fig. 1 Structure of the $[Mn(HC_4O_4)_2(OH_2)_4]$ molecular building block. All non-hydrogen atoms are presented as 50% thermal ellipsoids and all hydrogen atoms by open spheres for clarity

The delocalized electronic structure appears to be retained since the C–C bond lengths and angles of the bound ligand are essentially unchanged relative to those observed for the squarate dianion present in $K_2(C_4O_4)\cdot H_2O$ crystals.[11] Also, the Mn–O(1)–C(1) angle of 163.1(1)° is approaching 180° instead of < 120° as expected for a bent oxygen. Infrared data show only a small shift in ν(C=O) of bound squarate monoanion (1815 cm^{-1}) from that observed in free squarate (1822 cm^{-1}).[12] The arrangement of the building unit in the solid is shown in Fig. 2, where the six symmetry inequivalent oxygens [O(1), O(2), O(3), O(4), O(5) and O(6)] act as recognition sites to its organization in the crystal. One of the most notable features of the structure is the formation of very strong and what appears to be symmetrical O–H ··· O interactions. These are similar to the hydrogen bonds observed in a number of species such as HF_2^- and $H(RCO_2)_2^-$ containing very acidic hydrogens.[13a] They compare well with the crystallographically symmetrical bonds

Table 2 Atomic coordinates (× 10^4) for $[Mn(HC_4O_4)_2(OH_2)_4]$ **1** and $[Zn(C_4O_4)(OH_2)_2(dmso)_2]$ **2** with estimated standard deviations in parentheses

Atom	*x*	*y*	*z*
1			
Mn	5 000	5 000	5 000
C(5)	7 741(2)	3 159(2)	6 743(1)
O(6)	3 161(2)	2 385(2)	5 640(1)
C(1)	8 984(3)	3 202(2)	2 183(2)
O(1)	7 644(2)	4 160(2)	3 051(1)
C(2)	8 695(3)	3 000(2)	673(2)
O(2)	6 904(2)	3 741(2)	−307(1)
C(3)	11 293(3)	1 715(2)	646(2)
O(3)	12 703(2)	886(2)	−352(1)
C(4)	11 678(3)	1 863(2)	2 178(2)
O(4)	13 486(2)	1 224(2)	3 058(1)
2			
Molecule 1			
Zn(1)	0	5 000	5 000
O(1)	−144(3)	2 633(4)	5 571(4)
O(2)	−364(3)	−925(5)	6 523(4)
C(1)	−64(4)	1 209(7)	5 251(5)
C(2)	−169(4)	−417(6)	5 680(6)
S(1)	2 025(1)	3 418(2)	6 604(2)
O(3)	1 458(3)	5 011(4)	6 274(4)
C(3)	2 438(6)	3 216(8)	8 197(7)
C(4)	3 116(5)	3 900(12)	6 580(9)
O(4)	−372(3)	5 807(5)	6 348(4)
Molecule 2			
Zn(2)	5 000	0	0
O(21)	4 770(3)	2 390(4)	540(4)
O(22)	4 470(3)	6 028(4)	1 342(4)
C(21)	4 899(4)	3 818(6)	231(5)
C(22)	4 763(4)	5 475(6)	607(5)
S(21)	3 006(1)	−1 961(2)	−1 493(2)
O(23)	3 516(3)	−474(5)	−728(4)
C(23)	2 472(7)	−1 303(11)	−3 027(8)
C(24)	1 978(6)	−2 179(12)	−1 268(9)
O(24)	5 201(4)	−882(6)	1 677(4)

Table 3 Selected interatomic distances (Å) and angles (°) for $[Mn(HC_4O_4)_2(OH_2)_4]$ **1** and $[Zn(C_4O_4)(OH_2)_2(dmso)_2]$ **2**

1		**2**	
Mn–O(1)	2.151(1)	Zn(1)–O(1)	2.089(4)
Mn–O(5)	2.143(1)	Zn(1)–O(3)	2.134(4)
Mn–O(6)	2.221(1)	Zn(1)–O(4)	2.078(6)
C(1)–O(1)	1.233(2)	C(1)–O(1)	1.244(7)
C(2)–O(2)	1.281(2)	C(2)–O(2)	1.264(10)
C(3)–O(3)	1.268(2)	C(1)–C(2)	1.455(8)
C(4)–O(4)	1.232(2)	C(1)–C(2c)	1.484(10)
C(1)–C(2)	1.454(3)	O(4)–H(1)	0.96(6)
C(2)–C(3)	1.432(2)	O(4)–H(2)	0.85(8)
C(3)–C(4)	1.471(3)		
O(1)–Mn–O(1a)	180.0(1)	O(1)–Zn(1)–O(4)	180.0(1)
O(1)–Mn–O(5)	91.9(1)	O(4)–Zn(1)–O(3b)	89.8(2)
O(1)–Mn–O(5a)	88.1(1)	O(1)–Zn(1)–O(3)	89.9(1)
O(1)–Mn–O(6)	89.9(1)	O(1)–Zn(1)–O(3b)	90.1(1)
O(1)–Mn–O(6a)	91.0(1)	O(3)–Zn(1)–O(4)	90.2(2)
O(5)–Mn–O(6)	87.8(1)	O(1)–Zn(1)–O(1b)	180.0(–)
O(5)–Mn–O(6a)	92.2(1)	Zn(1)–O(1)–C(1)	135.2(5)
Mn–O(1)–C(1)	163.1(1)	O(1)–C(1)–C(2)	133.5(7)
C(1)–C(2)–C(3)	91.7(1)	O(1)–C(1)–C(2c)	137.3(6)
C(2)–C(3)–O(3)	133.9(1)	O(2)–C(2)–C(1)	133.9(6)
C(1)–C(4)–O(4)	135.0(2)	O(2)–C(2)–C(1b)	135.3(5)
		C(2)–C(1)–C(2c)	89.3(5)
		Zn(1)–O(3)–S(1)	120.5(2)
		Zn(1)–O(4)–H(1)	103(6)
		Zn(1)–O(4)–H(2)	125(7)

Symmetry operations: a $-x, -y, 1-z$; b $x, -1+y, z$; c $-x, 1-y, 1-z$.

reported for $Li(HC_4O_4)\cdot H_2O$ [2.431(1) Å] and $[H_2NMe_2][H_3(C_4O_4)_2]$ [2.435(2) Å].[13b,c] In the manganese compound, there are two such interactions, namely O(2)–H(2)···O(2) [2.481(1) Å] and O(3)–H(3)···O(3) [2.464(1) Å]; these are the strongest hydrogen-bonding interactions in the structure, and they are significantly shorter than those present in ice [2.752(8) and 2.765(0.2) Å].[14] The presence of such interactions is also indicated by the appearance of two transmission windows in the infrared spectrum occurring at 834 and 645 cm^{-1}, which are found to be in agreement with those observed for a similar arrangement in $K(HC_4O_4)\cdot H_2O$.[15] The formation of an extended chain resulting from O(2)–H(2)···O(2) interactions is shown in Fig. 2(*a*), and their aggregation to a sheet [Fig. 2(*b*)] by virtue of the O(3)–H(3)···O(3) interactions is fundamental to the formation of a strongly associated structural arrangement. The assembly of the chains into sheets is reinforced by two symmetry equivalent interactions resulting from the ability of the aqua oxygen [O(5)] to act as a hydrogen-bond donor to O(3) of an adjacent chain with O(5)–H···O(3) = 2.751(1) Å. In the overall structure [Fig. 2(*c*)], the remaining aqua molecules [labelled O(6) and O(6a) in Fig. 1] serve as junctions linking adjacent sheets *via* two sets of three hydrogen-bonded interactions [two O(6)–H···O(4) and one O(5)–H···O(6)] of comparable strength to O(5)–H···O(3). In this way, the void structure that is apparent in the sheet arrangement is filled with two aqua $O(6)H_2$ molecules, one from a sheet above and the other from a sheet below, to give a closely associated hydrogen-bonded network.

Structure of $[Zn(C_4O_4)(OH_2)_2(dmso)_2]$ **2**.—The complexity of the hydrogen-bonded network just described can be significantly reduced by employing dmso as a solvent. The reaction of $Zn(NO_3)_2\cdot 6H_2O$ with an equimolar amount of $H_2C_4O_4$ in dmso yields crystalline $[Zn(C_4O_4)(OH_2)_2(dmso)_2]$, which was formulated by total elemental analysis and identified by a single-crystal X-ray diffraction determination. Crystal data, atomic coordinates and selected bond lengths and angles are given in Tables 1–3, respectively. The zinc(II) ion is bound to two squarate dianions, two water and two dmso molecules in an almost perfect octahedron as shown in Fig. 3. The asymmetric unit contains two crystallographically independent units that only differ in the torsion angle that the squarate ligand makes with the plane containing the zinc, water and the two squarate oxygens co-ordinated to the zinc [O(4)–Zn(1)–O(1)–C(1) = 178.9(0.5)° and O(24)–Zn(1)–O(24a)–C(25a) = 152.1(0.4)° for the two crystallographically distinct molecules].

The structure shown in Fig. 4 reveals that it is a hydrogen-bonded layered solid, made up of 1 : 1 chains of zinc to squarate, where the zinc ions and the centres of the squarates all lie on the same line. The presence of such chains is very common for the totally hydrated metal squarates, however these tend to have weak but extensive hydrogen-bonding interactions leading to three-dimensional networks.[10] In this compound only two interactions hold the chains together: $O(4)H_2$ acts as a hydrogen-bond donor to O(2) of a squarate within the chain [O(4)–H(2)···O(2) = 2.646(6) Å] and to another oxygen [O(2)] in an adjacent chain [O(4)–H(2)···O(2b) = 2.735(6) Å], which leads to the formation of a hydrogen-bonded layer. As a consequence of the dmso ligands binding axially to zinc, the sheets are prevented from further aggregation to form a three-dimensional network.

Conversion Reactions.—These reactions are summarized in Scheme 1. The molecular $[Mn(HC_4O_4)_2(OH_2)_4]$ is tightly held in the solid state by hydrogen-bonding interactions which prevent its dissociation in solution and contribute to its insolubility in water and common organic solvents at room-temperature. However, in boiling water the hydrogen bonds can be disrupted and the solid is dissolved, which upon cooling recrystallizes into the original structure with the integrity of the manganese building-block complex maintained as confirmed by XRD.

When a pure solid sample of this compound is placed in warm water for only 1 h it was heterogeneously converted to a white solid which was identified by XRD as the $Mn(C_4O_4)(OH_2)_2$ phase reported earlier.[4] This compound possesses an interesting structure which is composed of a three-dimensional cage network with the metal ions linked octahedrally by four squarate ligands and two *trans* water molecules. The overall structure of this phase (centre of Scheme 1) may be viewed as made up of cubes sharing faces, with each cube representing a cage that is composed of metal ions occupying its edges and squarate ligands occupying its faces. The water molecules are bound to the metal centres and thus are suspended into the cavities caused by the formation of these cages. The squarate in this compound is bound through all its oxygens to four different metal centres and the infrared spectrum shows one band at 1525 cm^{-1} where ν(C=O), ν(C=C), ν(C–C, C–O) are expected to appear. This is in contrast to several bands, observed in that region, for $[Mn(HC_4O_4)_2(OH_2)_4]$ and $[Zn(C_4O_4)(OH_2)_2(dmso)_2]$, where one and two squarate oxygens are bound to the manganese and zinc atoms, respectively.

The isomorphous phase $Zn(C_4O_4)(OH_2)_2$ was also achieved by simply stirring crystalline $[Zn(C_4O_4)(OH_2)_2(dmso)_2]$ in water at room temperature. While we do not know the course of these conversion reactions, their outcome indicates that condensation of the molecular $[Mn(HC_4O_4)_2(OH_2)_4]$ and cross-linking of the $[Zn(C_4O_4)(OH_2)_2(dmso)_2]$ chains might be a plausible pathway for the formation of the ultimate cage-containing network.

Using a similar procedure to that reported, the three-dimensional cage network $Zn(C_4O_4)(OH_2)_2$ was prepared but as the pyridine adduct. This was done by neutralizing a solution of zinc nitrate and squaric acid with pyridine. Its XRD pattern was found to be in agreement with that calculated using the single-crystal diffraction data obtained from ref. 4. Elemental microanalysis on several samples prepared with pyridine showed consistently the presence of 0.2 pyridine molecules per

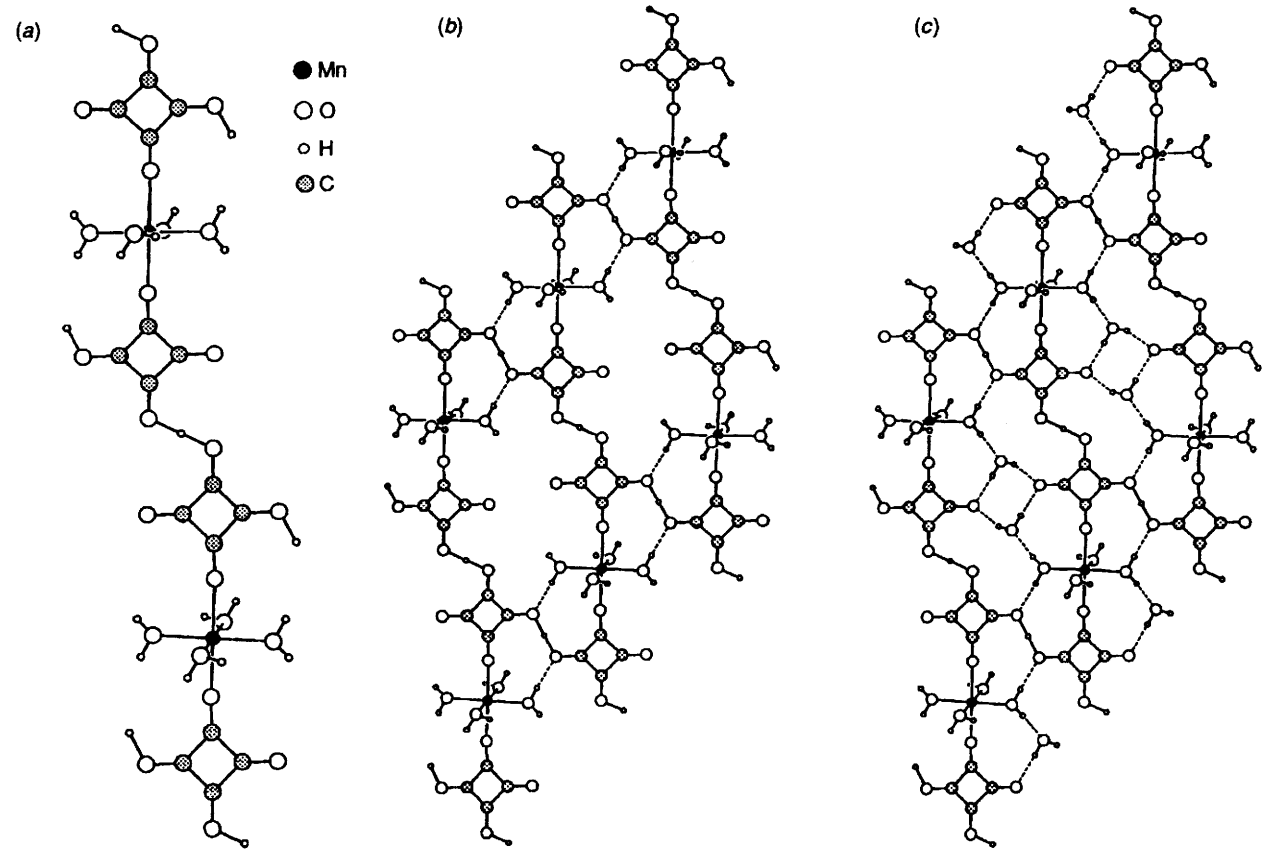

Fig. 2 Plots showing hydrogen-bonding interactions in crystalline $[Mn(HC_4O_4)_2(OH_2)_4]$ and their function in organizing the solid structure. The orientation and atom-labelling scheme used in Fig. 1 applies here. The short and possibly symmetric interactions, O(2)–H(2)···O(2) and O(3)–H(3)···O(3), which are respectively drawn as solid lines to H(2) and H(3), form an extended chain (*a*) and a sheet structure (*b*). The longer and more extensive interactions, which are shown as dotted lines originating from the metal centre, not only act to enforce the sheet organization but also to cause its aggregation with adjacent sheets (only water molecules of these sheets are drawn for clarity) to produce a tightly held three-dimensional network (*c*)

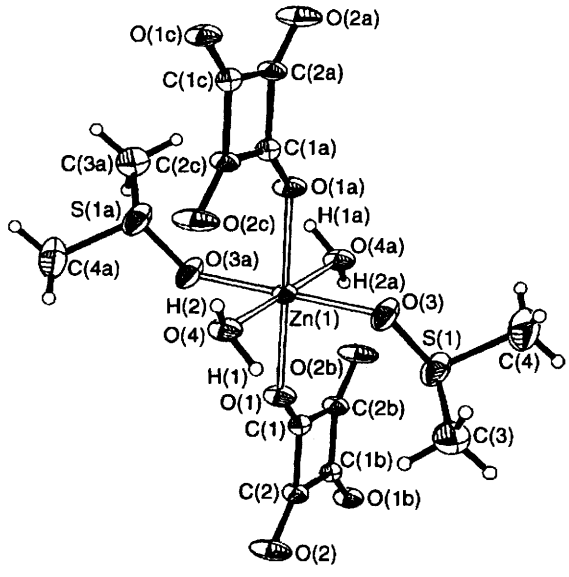

Fig. 3 Structure of one of the two crystallographically independent units found in the $[Zn(C_4O_4)(OH_2)_2(dmso)_2]$ crystal. The metal of unit 2 [Zn(2)] occupies a crystallographic inversion centre in the lattice at $\frac{1}{2}$, 0, 0. All non-hydrogen atoms are represented as 50% thermal ellipsoids and all hydrogen atoms by open spheres for clarity

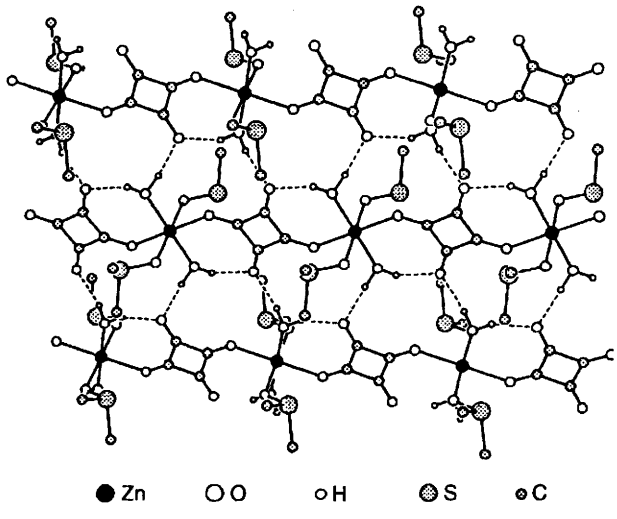

Fig. 4 Plot of the hydrogen-bonding arrangement existing between the chains of crystalline $[Zn(C_4O_4)(OH_2)_2(dmso)_2]$

metal ion, in spite of their treatment under vacuum for 48 h. We have not yet fully established the pyridine position and its orientation within the framework, however solid-state ^{13}C NMR spectra show three singlet peaks due to the *ortho*-, *meta*- and *para*-carbon atoms of pyridine at chemical shift values that are in agreement with those reported for free pyridine molecules included in the silicate cavities of dodecasil-3C ($17SiO_2 \cdot C_5H_5N$).[16a] In addition, a more intense and sharp singlet peak due to the squarate has been observed, perhaps due to polarization transfer from adjacent water protons. Currently, we are attempting to include other organic molecules of a highly polarizable nature for the possibility of achieving non-linear effects as observed in silicate-based host frameworks.[16]

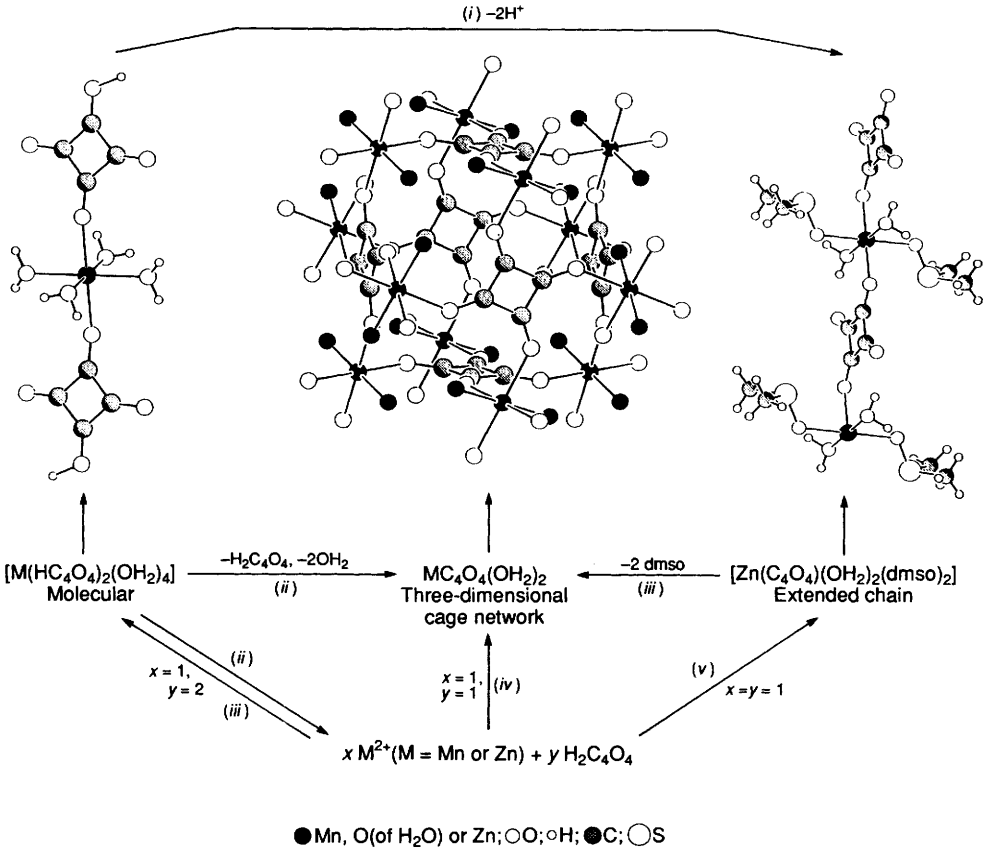

Scheme 1 Conversion reactions of the chain-containing complexes $[Mn(HC_4O_4)_2(OH_2)_4]$ and $[Zn(C_4O_4)(OH_2)_2(dmso)_2]$ to the three-dimensional cage network of the $M(C_4O_4)(OH_2)_2$ phase (M = Mn or Zn) (plot prepared using single-crystal data from ref. 4) (*i*) M^{2+}, dmso, 25 °C; (*ii*) water, 100 °C; (*iii*) water, 25 °C; (*iv*) water, 80 °C; (*v*) dmso, 25 °C

Conclusion

The complex hydrogen-bonded network of the molecular solid $[Mn(HC_4O_4)_2(OH_2)_4]$ can be simplified by utilizing dmso to block some of the hydrogen-bonding sites and lead to the formation of the extended hydrogen-bonded sheet $[Zn(C_4O_4)(OH_2)_2(dmso)_2]$. These compounds are insoluble in water and organic solvents due to hydrogen-bonding interactions acting collectively over a wide surface area which not only impart overall stability to the crystal, but also provide opportunities for directing and expressing some control over the structural progression of the solid framework.

These compounds undergo facile and clean conversion reactions to produce a three-dimensional extended cage system containing cavities where water molecules are anchored. This finding provides an easy pathway connecting molecular and chain-like solids of this kind to three-dimensional covalent systems with voided topology, which points to the possibility of *in situ* reactions aimed at incorporating a wide range of metal fragments or molecular entities within the ultimate structure.

Experiments addressing these issues, and focusing on the impact of these findings on the preparation of new open-framework compounds using these and similar molecular building blocks, are in progress.[17]

Acknowledgements

This work was partially supported by the National Science Foundation grant CHE-9224279.

References

1 See *ACS Symp. Ser.*, 1992, **499**; P. J. Fagan and M. D. Ward, *Sci. Am.*, 1992, **267**, 48; T. E. Mallouk and H. Lee, *J. Chem. Educ.*, 1990, **67**, 829.
2 O. M. Yaghi, Z. Sun, D. A. Richardson and T. L. Groy, *J. Am. Chem. Soc.*, 1994, **116**, 807.
3 G. A. Jeffrey and W. Saenger, *Hydrogen Bonding In Biological Structures*, Springer, Berlin, 1991; J. M. Lehn, *Angew. Chem., Int. Ed. Engl.*, 1990, **29**, 1304; J. A. Zerkowski, C. T. Seto, D. A. Wierda and G. M. Whitesides, *J. Am. Chem. Soc.*, 1990, **112**, 9025.
4 A. Weiss, E. Riegler and C. Roble, *Z. Naturforsch., Teil B*, 1986, **41**, 1333.
5 SHELXTL PC (Release 4.1), XPOW, Siemens, Madison, WI, 1990.
6 G. M. Sheldrick, SHELXTL PLUS (Release 4.0), Siemens, Madison, WI, 1990.
7 SHELXTL PC (Release 4.1), XEMP, Siemens, Madison, WI, 1990.
8 G. M. Sheldrick, SHELXTL PC (Release 4.1), XS, Siemens, Madison, WI, 1990,
9 G. R. Desiraju, *Crystal Engineering: The Design Of Organic Solids*, Elsevier, New York, 1989, pp. 115–173.
10 G. M. Frankenbach, M. A. Beno, A. M. Kini, J. M. Williams, U. Welp, J. E. Thompson and M. H. Whangbo, *Inorg. Chim. Acta*, 1992, **192**, 195; C. Roble and A. Weiss, *Z. Naturforsch., Teil B*, 1986, **41**, 1341; A. Weiss, E. Riegler and C. Roble, *Z. Naturforsch., Teil B*, 1986, **41**, 1329; A. Weiss, E. Riegler, I. Alt, H. Böhme and C. Roble, *Z. Naturforsch., Teil B*, 1986, **41**, 18; J. A. C. Van Ooijen, J. Reedijk and A. L. Spek, *Inorg. Chem.*, 1979, **18**, 1184.
11 W. M. Macintyre and M. S. Werkema, *J. Chem. Phys.*, 1964, **42**, 3563.
12 F. G. Baglin and C. B. Rose, *Spectrochim. Acta, Part A*, 1970, **26**, 2293.
13 (*a*) J. Emsley, *Chem. Soc. Rev.*, 1980, 91; (*b*) D. Semmington, *Acta Chem. Scand., Ser. A*, 1976, **30**, 808; (*c*) Y. Wang and G. D. Stucky, *J. Chem. Soc., Perkin Trans. 2*, 1974, 925.
14 S. W. Peterson and H. A. Levy, *Acta Crystallogr.*, 1957, **10**, 70.
15 D. P. C. Thackeray and B. C. Stace, *Spectrochim. Acta, Part A*, 1974, **30**, 1961.
16 (*a*) H. K. Chae, W. G. Klemperer, D. A. Payne, C. T. A. Suchicital, D. R. Wake and S. R. Wilkson, *ACS Symp. Ser.*, 1991, **455**, 528; (*b*) H. Gies, in *Inclusion Compounds: Inorganic and Physical Aspects of Inclusion*, eds. J. L. Atwood, J. E. D. Davies and D. D. MacNicol, Oxford Science Publications, New York, 1991, vol. 5, pp. 1–31.
17 O. M. Yaghi and G. Li, 207th National Meeting of the American Chemical Society, San Diego, 1994, Abstracts of Papers, INOR-533.

Received 7th July 1994; *Paper* 4/04148H